acid zwitterions, but it seems unlikely that this factor would explain the 35-fold difference in k_1 for methyl oxalate and chloroacetate.

The slower reactions observed with oxalate and methyl oxalate are clearly related to further anation, because the product is the bis(oxalato) complex. However, the kinetics reveal that these are not just simple complexation reactions, and they have been assigned to chelate ring closing and isomerization. Similar bis-complex formation was observed in the hypophosphite system,[6] which also required an isomerization step.

It is noteworthy that complexing of methyl oxalate to $(H_2O)_5CrCH_2CN^{2+}$ results in ester hydrolysis at a rate much greater than that of the free ester. This type of intramolecular rate acceleration could be an important property of these alkylchromium complexes and is being investigated further.

Experimental Section

Solutions of $(H_2O)_5CrCH_2CN^{2+}$ and standard reagents were prepared as described previously.[6,17] The low solubility of zinc(II) oxalate required the use of zinc-free chromium solutions that were prepared from chromium metal (99.999% United Mineral & Chemical Corp.) and perchloric acid. Ionic strength was maintained with $LiClO_4$.

Lithium oxalate was made by treating a saturated solution of oxalic acid at 65 °C with Li_2CO_3. The warm solution was filtered, reduced to one third of its volume, and cooled in ice. The white solid was collected and dried in vacuum over silica gel. Anal. Calcd for $Li_2C_2O_4$: C, 23.57; H, O. Found: C, 23.32; H, 0.04.

Sodium methyl oxalate was prepared by hydrolysis of dimethyloxalate[18] following the method of Skrabal[14] for the potassium salt. The sodium salt is much less soluble than the potassium salt in methanol, and it was not recrystallized. The product was identified as >99.6% $NaO_2C_2O_2CH_3$ by both saponification and permanganate analyses. The ^1H NMR spectrum in D_2O shows a singlet at 3.90 ppm vs. external Me_4Si.

Solutions of $(C_2O_4)Cr(OH_2)_4^+$ and *cis*-$(C_2O_4)_2Cr(OH_2)_2^-$ were prepared as described by Schenck et al.[19] Solid *cis*-$Na[(C_2O_4)_2Cr(OH_2)_2]$ was prepared by the method of Werner.[20]

Sodium trifluoroacetate was prepared by adding Na_2CO_3 to aqueous CF_3CO_2H and then evaporating the solution on a steam bath until white solid began to appear. Then 2-butanol was added until the solution became cloudy, and the mixture was cooled in ice. The white solid was collected by filtration, washed with ether, and dried over silica gel. Anal. Calcd for $NaO_2C_2F_3$: C, 17.66, H, O. Found: C, 17.59; H, 0.09.

Acid Dissociation Constant of $CH_3O_2C_2O_2H$. The absorbance of solutions of $NaO_2C_2O_2CH_3$ was monitored at 240 nm as a function of added $HClO_4$. The results were analyzed by an iterative least-squares method, which corrected for the amount of bound H^+ and gave $K_a = (7.04 \pm 0.24) \times 10^{-2}$ M at 25 °C.

Product Analysis. In the study with oxalate, the Cr:oxalate ratio was determined in the product after ion-exchange separation. Chromium was determined spectrophotometrically as chromate after oxidation with alkaline hydrogen peroxide. The oxalate was liberated from the chromium(III) by treatment with solid NaOH followed by acidification with glacial acetic acid. However blank experiments with known amounts of chromium(III) and oxalate revealed that one oxalate per chromium was always held back, and results were corrected for this fact. The oxalate was too dilute to determine by standard permanganate titration, so that the spectrophotometric method described by Burriel-Marti et al.[21] was used.

Instrumentation. The stopped-flow system is described elsewhere.[6,22] Spectrophotometric measurements were done on a Cary 219 spectrophotometer except for a few kinetic studies on a Hewlett-Packard 8451 diode-array system.

Acknowledgment. The authors acknowledge the financial support of the Natural Sciences and Engineering Research Council of Canada.

Registry No. $(H_2O)_5CrCH_2CN^{2+}$, 76068-68-3; $NH_3CH_2CO_2^-$, 56-40-6; $^+N(CH_3)_3CH_2CO_2^-$, 107-43-7; $ClCH_2CO_2^-$, 14526-03-5; $CF_3CO_2^-$, 14477-72-6; $HO_2C_2O_2^-$, 920-52-5; $CH_3O_2C_2O_2^-$, 44546-01-2.

---

(17) Kupferschmidt, W.; Jordan, R. B. *J. Am. Chem. Soc.* **1984**, *106*, 991.

(18) Bowden, E. *Organic Syntheses*; Wiley: New York, 1941; Collect. Vol. 2, p 414.

(19) von Schenk, C.; Steiger, H.; Kelm, H. *Z. Anorg. Allg. Chem.* **1972**, *391*, 1.

(20) Werner, A. *Justus Liebigs Ann. Chem.* **1914**, *406*, 304.

(21) Burriel-Marti, F.; Ramirez-Munoz, J.; Fernandez-Caldas, E. *Anal. Chem.* **1953**, *25*, 583.

(22) Pinnell, D.; Jordan, R. B. *Inorg. Chem.* **1979**, *18*, 3595.

Contribution from the Institute for Physical and Theoretical Chemistry,
University of Frankfurt, 6000 Frankfurt/Main, Federal Republic of Germany

Formation and Reactivity of Palladium(II) Sulfito Complexes in Aqueous Solution. 2. Kinetics and Mechanisms

G. Mahal and R. van Eldik*

Received November 19, 1986

The kinetics of the formation of $Pd(Et_4dien)SO_3$ (Et_4dien = 1,1,7,7-tetraethyldiethylenetriamine) via the reaction of $Pd(Et_4dien)OH_2^{2+}$ with HSO_3^-/SO_3^{2-} was studied in detail as a function of pH, [total S], temperature, and pressure. The observed rate law excludes the possibility of SO_2 uptake by $Pd(Et_4dien)OH^+$ and favors an anation mechanism that involves a rapid encounter complex formation preequilibrium. The rate law and activation parameters support an associative reaction mode. On acidification to pH <6, the $Pd(Et_4dien)SO_3$ species undergoes complete loss of the Et_4dien ligand, and the reaction is characterized by a typical two-term rate law, $k_{obsd} = k_a + k_b$[total S]. The k_a path exhibits a characteristic pH dependence and reaches a limiting value of 5×10^{-3} s^{-1} at 25 °C and 0.5 M ionic strength with $\Delta H^* = 78 \pm 5$ kJ mol^{-1}, $\Delta S^* = -26 \pm 17$ J K^{-1} mol^{-1}, and $\Delta V^* \approx 0$. These data are discussed in terms of a rate-determining ring-opening reaction of the Et_4dien ligand. In strongly acidic medium, partial loss of the sulfite ligand occurs to produce the corresponding aquo complex, and the observed rate constant exhibits a linear dependence on $[H^+]$. Kinetic data for the dechelation reaction measured under conditions where the $Pd(Et_4dien)SO_3$ complex is produced in acidic medium via anation of the aquo complex are in good agreement with those measured with the pH-jump method described before. The results of this study are discussed in terms of the general substitution behavior of Pd(II) complexes and the labilization effect of coordinated sulfite.

Introduction

In part 1 of this study[1] a detailed spectroscopic (UV-vis, IR, and NMR) investigation of the overall reactions was performed. The results enabled a qualitative description of the formation and decomposition processes in terms of characterized intermediate and product species. In this study we have performed a detailed kinetic analysis of the system and can now present a quantitative description of the reactions. Similar mechanistic studies[2-12] have

---

*To whom all correspondence should be addressed at the Institute for Inorganic Chemistry, University of Witten/Herdecke, 5810 Witten-Annen, FRG.

(1) Mahal, G.; van Eldik, R. *Inorg. Chem.* **1987**, *26*, 1837.

(2) van Eldik, R.; Harris, G. M. *Inorg. Chem.* **1980**, *19*, 880.

(3) El-Awady, A. A.; Harris, G. M. *Inorg. Chem.* **1981**, *20*, 1660, 4251.

(4) Dash, A. C.; El-Awady, A. A.; Harris, G. M. *Inorg. Chem.* **1981**, *20*, 3160.

0020-1669/87/1326-2838$01.50/0 © 1987 American Chemical Society

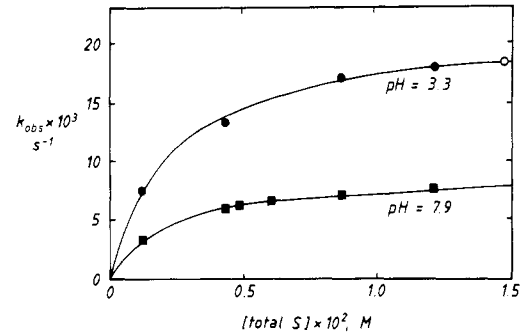

Figure 1. Dependence of k_{obsd} on [total S] at different pHs for the anation of $Pd(Et_4dien)OH_2^{2+}$ by sulfite. Conditions: [Pd] = 8.7×10^{-5} M; temperature 25 °C; ionic strength 0.5 M.

revealed interesting aspects in the past and in general have added to the better understanding of the fundamental chemistry involved. In this respect it is important to mention the identification and kinetic behavior of O-bonded sulfito complexes and the possible role they could play in metal-catalyzed oxidation reactions of S(IV).[13] The fact that we have now identified a system in which coordinated sulfite can labilize a chelated amine adds a further dimension to such reactions and the understanding of their general behavior.

Experimental Section

Materials. Details on the preparation of the complexes and chemicals used are given in part 1 of this study.[1]

Measurements. UV-vis absorption spectra were recorded on the instruments mentioned before. These spectrophotometers were all equipped with thermostated (±0.1 °C) cell holders that enabled the kinetic measurements to be made at ambient pressure. A modified Zeiss PMQ II spectrophotometer equipped with a thermostated (±0.1 °C) high-pressure cell,[14] suitable to hold the pillbox sample cell,[15,16] was used for the kinetic measurements at high pressure. An Aminco stopped-flow and a specially designed high-pressure stopped-flow unit[16,17] were used to study the more rapid reactions. The acid dissociation constant of $Pd(Et_4dien)OH_2^{2+}$ was measured spectrophotometrically and found to be (pK_a) 7.4 at 25 °C and 0.5 M ionic strength.[18]

Results and Discussion

Formation of $Pd(Et_4dien)SO_3$. The spectral observations reported in part 1 of this series[1] demonstrated that $Pd(Et_4dien)SO_3$ is produced as a stable reaction product during the anation of $Pd(Et_4dien)OH_2^{2+}$ by sulfite at pH ≥7 and as an intermediate species during the same reaction at pH <7. The kinetics of the formation reaction can be followed either at the absorption maximum of $Pd(Et_4dien)SO_3$ at 271 nm for pH ≥7 or at the isosbestic point around 262 nm (depending on pH and sulfite concentration), where the subsequent decomposition reaction does not interfere with the formation process. The extent to which the sulfito complex is produced in acidic medium depends on the rate of the formation reaction relative to that for the subsequent dechelation process. Pseudo-first-order rate constants for the formation reaction in the presence of excess sulfite were measured as a function of sulfite concentration at various pHs, temperatures, and pressures.[18] A summary of two representative series of data is given in Figure 1, from which it follows that k_{obsd} increases nonlinearly with [total S]. The curves do not exhibit a meaningful intercept and reach a limiting value at high [total S]. Furthermore, the data exhibit a strong pH dependence as shown in Figure 2.

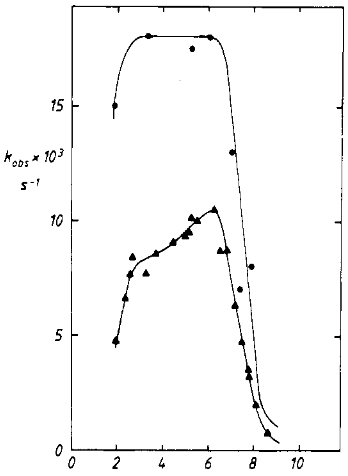

Figure 2. Dependence of k_{obsd} on pH at different [total S] for the anation of $Pd(Et_4dien)OH_2^{2+}$ by sulfite. Conditions: [Pd] = 8.7×10^{-5} M; temperature 25 °C; ionic strength 0.5 M; [total S] = 1.2×10^{-3} (▲) and 1.2×10^{-2} M (●).

Various data-fitting procedures were adopted[18] to determine the combined [total S]/pH dependence of k_{obsd}. The trends in Figures 1 and 2 can be interpreted qualitatively in the following way: The nonlinear [total S] dependence of k_{obsd} can be ascribed to the formation and kinetic participation of a precursor species which could be an ion-pair or encounter complex. A similar effect was observed in a recent study,[19] and it was suggested that the S(IV) species in solution, i.e. especially HSO_3^- and SO_3^{2-}, can produce an adduct with the coordinated amine ligand. This will show up as a preequilibrium step followed by a first-order interchange type of process, during which the actual anation reaction occurs. Such nonlinear dependencies can be linearlized by plotting k_{obsd}^{-1} vs. $[\text{total S}]^{-1}$, from which the precursor formation constant and the first-order interchange rate constant can be extracted. Preliminary data fitting demonstrated[18] that such curves go through a common intercept (interchange rate constant) and that the precursor formation constant increases with pH.

The pH dependence of k_{obsd} at a constant [total S] (Figure 2) results in a bell-shaped curve, which can be interpreted in terms of the $SO_2/HSO_3^-/SO_3^{2-}$ and $Pd(Et_4dien)OH_2^{2+}/Pd(Et_4dien)OH^+$ equilibria. At low pH, k_{obsd} decreases significantly due to the partial formation of SO_2, which cannot participate in the anation process. The increase in k_{obsd} with increasing pH is due to the higher nucleophilicity of SO_3^{2-} than of HSO_3^-. This is also clearly seen in the extent of which the $Pd(Et_4dien)SO_3$ species is produced under these conditions. The overall absorbance increase at 262 nm (isosbestic point) increases with pH and reaches a maximum at pH ~6, i.e. in agreement with the pH profile in Figure 2, indicating the efficiency of the formation reaction prior to the subsequent process (see further discussion). The falloff in k_{obsd} at pH >7 can be ascribed to the partial formation of the substitutionally inert $Pd(Et_4dien)OH^+$ species,[20] since the acid dissociation constant (pK_a) of the corresponding aquo complex was found to be 7.4 at 25 °C and 0.5 M ionic strength, which is in good agreement with that reported before.[21]

---

(5) van Eldik, R. *Inorg. Chim. Acta* **1980**, *42*, 49.
(6) Koshy, K. C.; Harris, G. M. *Inorg. Chem.* **1983**, *22*, 2947.
(7) van Eldik, R.; von Jouanne, J.; Kelm, H. *Inorg. Chem.* **1982**, *21*, 2818.
(8) Dasgupta, T. P.; Harris, G. M. *Inorg. Chem.* **1985**, *24*, 4399.
(9) Moritzen, P. A.; Harris, G. M.; El-Awady, A. A. *Inorg. Chem.* **1985**, *24*, 313.
(10) Kraft, J.; van Eldik, R. *Inorg. Chem.* **1985**, *24*, 3391.
(11) El-Awady, A. A.; Harris, G. M. *Inorg. Chem.* **1986**, *25*, 1323.
(12) van Eldik, R. *Adv. Inorg. Bioinorg. Mech.* **1984**, *3*, 275.
(13) van Eldik, R. In *Chemistry of Multiphase Atmospheric Systems*; Jaeschke, W., Ed.; Reidel: Dordrecht, The Netherlands, 1985; p 541.
(14) Fleischmann, F. K.; Conze, E. G.; Stranks, D. R.; Kelm, H. *Rev. Sci. Instrum.* **1974**, *45*, 1427.
(15) le Noble, W. J.; Schlott, R. *Rev. Sci. Instrum.* **1976**, *47*, 770.
(16) van Eldik, R. In *Inorganic High Pressure Chemistry: Kinetics and Mechanisms*; van Eldik, R., Ed.; Elsevier: Amsterdam, 1986; Chapter 1.
(17) van Eldik, R.; Palmer, D. A.; Schmidt, R.; Kelm, H. *Inorg. Chim. Acta* **1981**, *50*, 131.
(18) Mahal, G. Ph.D. Dissertation, University of Frankfurt, 1986.
(19) Joshi, V. K.; van Eldik, R.; Harris, G. M. *Inorg. Chem.* **1986**, *25*, 2229.
(20) Breet, E. L. J.; van Eldik, R.; Kelm, H. *Inorg. Chim. Acta* **1984**, *85*, 151.
(21) Breet, E. L. J.; van Eldik, R.; Kelm, H. *Polyhedron* **1983**, *2*, 1181.

Table I. Rate and Activation Parameters for the Reaction[a]

$Pd(Et_4dien)OH_2^{2+} + HSO_3^-/SO_3^{2-} \rightarrow Pd(Et_4dien)SO_3 + H_2O$

10^3[total S], M	temp, K	pressure, MPa	$10^3 k_{obsd}$,[b] s^{-1}	$\Delta H^\ddagger$, kJ mol^{-1}	$\Delta S^\ddagger$, J K^{-1} mol^{-1}	$\Delta V^\ddagger$, cm^3 mol^{-1}
1.23	288.2	0.1	2.75	70 ± 3	−4 ± 11	
	293.2		4.80			
	298.2		7.70			
	303.2		13.7			
	308.2		19.3			
	298.2	6	7.85			−10.4 ± 0.5
		25	8.80			
		50	9.50			
		75	10.7			
		100	11.8			
12.3	288.2	0.1	8.80	58 ± 5	−83 ± 5	
	293.2		13.0			
	298.2		18.0			
	303.2		31.0			
	308.2		44.0			
	298.2	5.5	22.9			−12.4 ± 0.6
		25	26.5			
		50	29.2			
		75	33.4			
		100	37.6			

[a] Conditions: [Pd(II)] = 8.7×10^{-5} M; pH 3.3; ionic strength 0.5 M. [b] Mean value of at least two kinetic experiments.

These kinetic trends can be employed to interpret the data in a quantitative way in terms of the following reaction mechanism. Equilibria 1–3 represent the various acid–base systems that form

$$H_2O + SO_2(aq) \overset{K_A}{\rightleftharpoons} HSO_3^- + H^+ \qquad (1)$$

$$HSO_3^- \overset{K_B}{\rightleftharpoons} SO_3^{2-} + H^+ \qquad (2)$$

$$Pd(Et_4dien)OH_2^{2+} \overset{K_C}{\rightleftharpoons} Pd(Et_4dien)OH^+ + H^+ \qquad (3)$$

$$Pd(Et_4dien)OH_2^{2+} + HSO_3^- \overset{K_1}{\rightleftharpoons} \{Pd(Et_4dien)OH_2^{2+} \cdot HSO_3^-\} \xrightarrow{k_1} Pd(Et_4dien)SO_3 + H_3O^+ \qquad (4)$$

$$Pd(Et_4dien)OH_2^{2+} + SO_3^{2-} \overset{K_2}{\rightleftharpoons} \{Pd(Et_4dien)OH_2^{2+} \cdot SO_3^{2-}\} \xrightarrow{k_2} Pd(Et_4dien)SO_3 + H_2O \qquad (5)$$

an essential part of the reaction scheme, for which $K_A = 1.25 \times 10^{-2}$, $K_B = 5.0 \times 10^{-7}$, and $K_C = 4.0 \times 10^{-8}$ M at 25 °C and 0.5 M ionic strength.[2] Both reactions 4 and 5 include a precursor formation step followed by a rate-determining interchange or anation step. Since it is generally known that such hydroxo complexes are substitutionally inert,[20] only the aqua complex was considered as a reactive species. The rate law (6) for the

$$k_{obsd} = \left(\frac{k_1 K_1 [HSO_3^-] + k_2 K_2 [SO_3^{2-}]}{1 + K_1 [HSO_3^-] + K_2 [SO_3^{2-}]} \right) \left(\frac{[H^+]}{K_C + [H^+]} \right) \qquad (6)$$

mechanism outlined above was derived on the assumption that the precursor formation steps do not significantly affect the fraction of the complex present in the aqua form, i.e. as expressed by $[H^+]/(K_c + [H^+])$. In this expression $[HSO_3^-]$ and $[SO_3^{2-}]$ can be calculated from the expressions in (7).

$$[HSO_3^-] = K_A[H^+][\text{total S}]/\{[H^+]^2 + K_A[H^+] + K_A K_B\}$$
$$[SO_3^{2-}] = K_A K_B[\text{total S}]/\{[H^+]^2 + K_A[H^+] + K_A K_B\} \qquad (7)$$

The trends observed during the preliminary fitting of the data mentioned above[18] allow us to assume that $k_1 \approx k_2$ and $K_2 \approx 2K_1$, so that there are only two unknown constants in eq 6. The latter was rewritten in the form (8), from which it is now possible to

$$\{[HSO_3^-] + 2[SO_3^{2-}]\}^{-1} = k_1 K_1 [H^+]/k_{obsd}\,(K_C + [H^+]) - K_1 \qquad (8)$$

estimate k_1 and K_1 by plotting $\{[HSO_3^-] + 2[SO_3^{2-}]\}^{-1}$ vs. $[H^+]/k_{obsd}\,(K_C + [H^+])$. Such a plot is given in Figure 3 for all the available data[18] as a function of pH and [total S], from which it follows that within the experimental error limits and under the mentioned assumptions, the data can be fitted over a wide pH and [total S] range with eq 8, i.e. the simplified form of eq 6. From the intercept and slope of the line in Figure 3 it follows that k_1 ($=k_2$) = $(2.55 \pm 0.14) \times 10^{-2}$ s^{-1} and K_1 ($=0.5K_2$) = 400 ± 47 M^{-1} at 25 °C. These values are in close agreement with those found in the preliminary data-fitting procedure;[18] viz. k_1 ($=k_2$) = 2×10^{-2} s^{-1} and K_1 ($=0.5K_2$) = 500 M^{-1}. It is obviously the order of magnitude of these values that is primarily of interest. The values of K_1 and K_2 are such that they cannot be ascribed to ion-pairing effects. Some direct interaction of HSO_3^- and SO_3^{2-} with the chelated amine to produce a precursor complex is a likely possibility. In such a case the formation constant should increase with increasing basicity. It follows that the precursor formation equilibria are of kinetic significance, but due to a lack of further information on them, their thermodynamic meaning and the associated effect on the overall system and rate law are of minor importance.[22]

The temperature and pressure dependence of this reaction was studied at pH 3.3, i.e. where the pH profiles for low (Figure 2) and high[18] [total S] exhibit an almost pH-independent process. This is important since the variation in temperature and pressure may affect the pH, which could result in an additional change in k_{obsd} when the latter is very pH sensitive. The corresponding rate constants and activation parameters for the formation of $Pd(Et_4dien)SO_3$ at two [total S] values are summarized in Table I. Very similar results were found at pH 5.2,[23] where the reaction shows a minor pH dependence. At low [total S] at pH 3.3, eq 6 can be simplified to $k_{obsd} = k_1 K_1 [HSO_3^-]$ so that the observed activation parameters are a combination of those for k_1 and K_1. For instance, $\Delta V^\ddagger = \Delta \bar{V}(K_1) + \Delta V^\ddagger(k_1)$. At high [total S], eq

---

[22] Alternatively, if the effect of the precursor formation equilibria is taken into account, eq 6 is modified to

$$k_{obsd} = \frac{k_1 K_1 [HSO_3^-] + k_2 K_2 [SO_3^{2-}]}{1 + K_c/[H^+] + K_1 [HSO_3^-] + K_2 [SO_3^{2-}]}$$

This equation requires a somewhat different treatment of the kinetic data, but since most of the data were recorded at pH <7, this modification has no significant effect on the overall interpretation of the data.

[23] At pH 5.2 and [total S] = 1.2×10^{-2} M, $\Delta H^\ddagger$ = 66 ± 3 kJ mol^{-1}, $\Delta S^\ddagger$ = −56 ± 11 J K^{-1} mol^{-1}, and $\Delta V^\ddagger$ = −16.6 ± 0.9 cm^3 mol^{-1}. At pH 5.2 and [total S] = 1.2×10^{-3} M, $\Delta V^\ddagger$ = −11.5 ± 0.4 cm^3 mol^{-1} (data taken from ref 18).

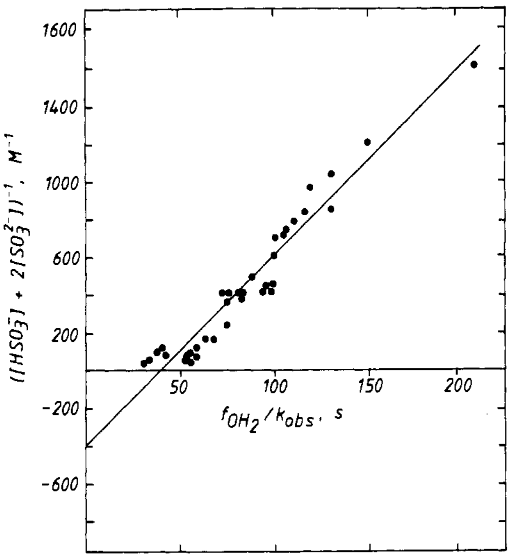

Figure 3. Plot of $([HSO_3^-] + 2[SO_3^{2-}])^{-1}$ vs. f_{OH_2}/k_{obsd} according to eq 8.

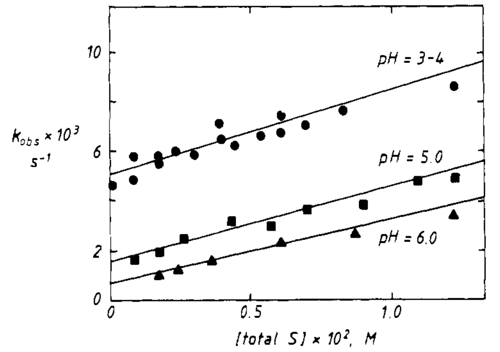

Figure 4. Dependence of k_{obsd} on [total S] at different pHs for the dechelation reaction of Pd(Et$_4$dien)SO$_3$ to produce Pd(SO$_3$)$_2^{2-}$. Conditions: [Pd] = 8.7 × 10^{-5} M; temperature 25 °C; ionic strength 0.5 M.

6 simplifies to $k_{obsd} = k_1$ and the activation parameters are those for k_1. The similarity in especially ΔV^* for these conditions indicates that $\Delta \bar{V}(K_1)$ is very small and that the observed ΔV^* is mainly that for $\Delta V^*(k_1)$. The negative sign of both ΔS^* and ΔV^* supports an associative reaction mode for the anation process. A comparison with anation rate data for closely related complexes[21,24] indicates that the reported activation parameters are in good agreement with an associative anation process. A similar conclusion was drawn from the data found at pH 5.2.[18,23]

The suggested mechanism outlined in reactions 1–5 excludes the possible formation of an O-bonded sulfito intermediate species. We did consider this possibility in the treatment of the data, but the observed pH dependence of the process, as well as the spectral observations reported in part 1, rule out this possibility. This trend is in good agreement with that observed for the reaction of such complexes with $CO_2/HCO_3^-/CO_3^{2-}$ to produce the corresponding carbonato species.[25] In the latter study the formation process follows the normal anation route via the aquo complex and no evidence for any CO_2 uptake by the hydroxo complex could be found. These results all point toward the peculiar nature of the Pd–OH moiety, which is substitutionally inert[20] but also not accessible via the uptake (addition) mechanism. This does question the nature of the Pd–OH bond in such complexes, and further investigations are presently under way in our laboratories.

Decomposition of Pd(Et$_4$dien)SO$_3$. The kinetics of this process can be followed conveniently by preparing Pd(Et$_4$dien)SO$_3$ at pH >7, where it is stable, and then acidifying the solution to low pH with the aid of a buffer. Such a pH jump results in the spontaneous dechelation reaction, which can be followed at 365 nm, the absorption maximum of Pd(SO$_3$)$_2^{2-}$. Typical kinetic results are reported as a function of [total S] and pH in Figures 4 and 5, respectively. In general, k_{obsd} increases with increasing [total S] and the slopes of such lines show no significant pH dependence except at low pH, where the slope almost disappears. This trend is ascribed to the formation of SO_2 under such conditions, which presumably cannot participate in the process to produce the Pd(SO$_3$)$_2^{2-}$ species. The pH independence of the slope demonstrates that the reaction with HSO_3^- and SO_3^{2-} occurs at the same rate. The intercepts of the plots in Figure 4 show a strong pH dependence, from which it follows that this term also accounts for the pH dependence at constant [total S] illustrated in Figure 5. The latter kinetic trends can be accommodated by the mechanism outlined in (9).

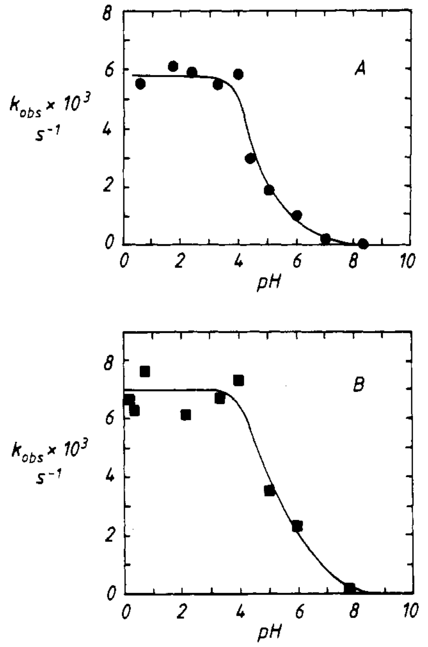

Figure 5. Dependence of k_{obsd} on pH at different [total S] for the dechelation reaction of Pd(Et$_4$dien)SO$_3$ to produce Pd(SO$_3$)$_2^{2-}$. Conditions: [Pd] = 8.7 × 10^{-5} M; temperature 25 °C; ionic strength 0.5 M; [total S] = 1.7 × 10^{-3} (A) and 6.1 × 10^{-3} M (B).

$$\mathrm{Pd(Et_4dien)SO_3 + H^+ \overset{K_D}{\rightleftharpoons} Pd(Et_4dien{\cdot}H^+)SO_3 \xrightarrow[+H_2O]{k_3}}$$
$$\mathrm{Pd(Et_4dien{\cdot}H^+)(H_2O)SO_3 \xrightarrow[+HSO_3^-/SO_3^{2-}]{fast}}$$
$$\mathrm{Pd(SO_3)_2^{2-} + Et_4dien{\cdot}H^+} \quad (9)$$

The mechanism accounts for the characteristic pH dependence of the process. The protonation of the coordinated Et$_4$dien ligand is followed by a rate-determining ring-opening (solvolysis) reaction to produce the aquo sulfito species, which rapidly dechelates in the presence of sulfite to produce the final products. The process is independent of [total S] and also accounts for the intercepts in Figure 4. It is comparable to the usual solvolysis path observed in substitution reactions of square-planar complexes, except that the process involves a protonated species. The Pd(Et$_4$dien)SO$_3$ complex cannot dechelate in the absence of H$^+$ (presumably to stabilize the released amine ligand), which accounts for the disappearance of this process at pH >7. On the other hand, protonation alone cannot account for the dechelation/solvolysis reaction and a significant labilization by the coordinated sulfite molecule must be taken into account (see part 1).[1] The overall rate law for the mechanism outlined in (9) is given in eq 10 and

$$k_{obsd} = k_3K_D[H^+]/\{1 + K_D[H^+]\} \qquad (10)$$

represents the [total S]-independent reaction path. At $[H^+] \gg$

---

[24] Kotowski, M.; van Eldik, R. In *Inorganic High Pressure Chemistry: Kinetics and Mechanisms*; van Eldik, R., Ed.; Elsevier: Amsterdam, 1986; Chapter 4.

[25] Mahal, G.; van Eldik, R. *Inorg. Chem.* **1985**, *24*, 4165.

Table II. Rate and Activation Parameters for the Reaction[a]

$$\mathrm{Pd(Et_4dien)SO_3} \xrightarrow[\mathrm{HSO_3^-}]{\mathrm{H^+}} \mathrm{Pd(SO_3)_2^{2-}} + \mathrm{Et_4dien{\cdot}}x\mathrm{H^+}$$

10^3[total S], M	temp, K	pressure, MPa	10^3k_{obsd},[b] s^{-1}	$\Delta H^‡$, kJ mol^{-1}	$\Delta S^‡$, J K^{-1} mol^{-1}	$\Delta V^‡$, cm^3 mol^{-1}
1.23	288.2	0.1	1.7	78 ± 5	−26 ± 17	
	293.2		3.1			
	298.2		6.3			
	303.2		7.3			
	308.2		15.4			
	313.2		27.1			
	298.2	6.5	6.1			~0
		28	6.2			
		52	6.2			
		75	6.1			
		100	6.2			
12.3	288.2	0.1	2.1	78 ± 3	−23 ± 10	
	293.2		3.6			
	298.2		7.7			
	303.2		12.2			
	308.2		19.6			
	313.2		30.5			
	298.2	6.2	6.0			~0
		23	6.0			
		49	6.1			
		77	5.9			
		100	6.0			

[a] Conditions: [Pd(II)] = 8.7×10^{-5} M; $\mathrm{Pd(Et_4dien)SO_3}$ complex prepared at pH 8.9 and acidified to pH 2.0; ionic strength 0.5 M. [b] Mean value of at least two kinetic experiments.

K_D^{-1}, eq 10 simplifies to $k_{obsd} = k_3$, which represents the limiting, acid-independent rate constant observed under such conditions (Figure 5). It follows that $k_3 = (5.8 \pm 0.5) \times 10^{-3}$ s^{-1} at [total S] = 1.75×10^{-3} M, 25 °C, and ionic strength 0.5 M. Similarly, K_D can be deduced from the sigmoid curve in Figure 5 and has a value of 4×10^4 M^{-1} under these conditions. This value is quite realistic if one considers the protonation constants for uncoordinated $\mathrm{Et_4dien}$,[26] viz. 4.6×10^9, 4.2×10^8, and 3.5×10^3 M^{-1}, and keeps in mind that coordinated ligands are usually significantly less basic than the free ligands by several orders of magnitude.[16]

The [total S] dependence, reported in Figure 4 can be interpreted as evidence for a direct-substitution route, during which $\mathrm{Pd(Et_4dien)SO_3}$ undergoes nucleophilic attack by $\mathrm{HSO_3^-/SO_3^{2-}}$ to produce the final species. This reaction exhibits no meaningful pH dependence, which indicates that neither the $\mathrm{HSO_3^-/SO_3^{2-}}$ equilibrium nor the protonation equilibrium presented by K_D has an effect on the direct-substitution pathway. This reaction can therefore be summarized as in (11), and the average value of k_4,

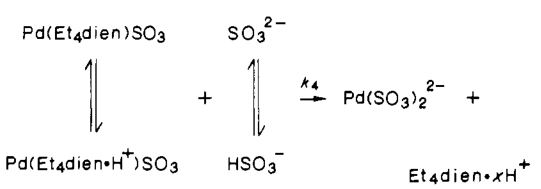

$$\begin{array}{c} \mathrm{Pd(Et_4dien)SO_3} \\ \Updownarrow \\ \mathrm{Pd(Et_4dien{\cdot}H^+)SO_3} \end{array} + \begin{array}{c} \mathrm{SO_3^{2-}} \\ \Updownarrow \\ \mathrm{HSO_3^-} \end{array} \xrightarrow{k_4} \mathrm{Pd(SO_3)_2^{2-}} + \mathrm{Et_4dien{\cdot}}x\mathrm{H^+} \quad (11)$$

calculated from the slopes of the lines in Figure 4, viz. 0.30, 0.26, and 0.22 M^{-1} s^{-1} for pH 3–4, 5.0, and 6.0, respectively, is 0.26 ± 0.04 M^{-1} s^{-1} at 25 °C and 0.5 M ionic strength. The slight decrease with increasing pH does point to some pH dependence of the various possible reactions that participate in the overall reaction (11). However, this effect is so small that it does not add to a better understanding of the system.

The reported results clearly demonstrate the strong labilization effect of coordinated sulfite.[27] Other closely related studies have reported similar effects,[10,28,29] but this is to our knowledge the first report in which coordinated sulfite is capable of dechelating an usually strongly bonded amine ligand. Subsequent reactions of the $\mathrm{Pd(SO_3)_2^{2-}}$ species to produce $\mathrm{Pd(SO_3)_3^{4-}}$ or even more highly substituted forms are non-rate-determining steps, so that the reaction products (palladium sulfito species) show up in an equilibrium ratio depending on the pH and [total S] of the reaction mixture.

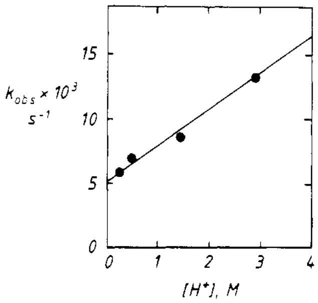

Figure 6. Dependence of k_{obsd} on [H+] for the dechelation/aquation of $\mathrm{Pd(Et_4dien)SO_3}$ in strongly acidic medium. Conditions: [Pd] = 8.7×10^{-5} M; temperature 25 °C; ionic strength 0.5 M; [total S] = 8.7×10^{-4} M.

Further information on the intimate nature of the reaction mechanisms for the acid-catalyzed "solvolysis" and direct nucleophilic substitution paths can be obtained from the activation parameters $\Delta H^‡$, $\Delta S^‡$, and $\Delta V^‡$. The temperature and pressure dependence of the decomposition process was studied on the plateau of the pH profile to exclude possible variations in the observed rate constants due to the effect of temperature and pressure on the pH of the solution. In addition, under the selected conditions (pH 2) no meaningful [total S] dependence exists and the results for different [total S] are very similar as seen from the data in Table II. Surprising is the fact that $\Delta S^‡$ and $\Delta V^‡$ are practically zero, in contrast to the usual negative values observed for such spontaneous solvolysis processes.[24] This is clearly in line with the labilization effect of the sulfite ligand which could introduce a dissociative reaction mode. It may therefore be quite realistic to think in terms of a pure interchange mechanism in which bond rupture (ring opening of the $\mathrm{Et_4dien}$ ligand) is accompanied by bond formation with either a solvent molecule or a sulfite ion. This difference is clearly seen from a comparison with rate and activation parameters for related reactions sum-

---

(26) Sillen, L. G. *Spec. Publ.—Chem. Soc.* **1971**, *No. 17*, 680.
(27) Mahal, G.; van Eldik, R. *J. Chem. Soc., Chem. Commun.* **1987**, 328.
(28) Spitzer, U.; van Eldik, R. *Inorg. Chem.* **1982**, *21*, 4008.
(29) Berger, J.; Kotowski, M.; van Eldik, R., unpublished results.

marized in Tables 4.1 and 4.2 of ref 24.

In strongly acidic medium, aquation of the sulfite ligand occurs in competition with dechelation (see part 1). The results in Figure 6 demonstrate a linear $[H^+]$ dependence for which the intercept coincides with the value of k_3 (maximum intercept in Figure 4). The results can be presented by eq 12, where k_b represents the

$$k_{obsd} = k_a + k_b[H^+] \qquad (12)$$

acid-catalyzed aquation reaction. Under these conditions the $Pd(Et_4dien)SO_3$ species is in the protonated form $Pd(Et_4dien{\cdot}H^+)SO_3$, and further protonation of the sulfite ligand, only expected to occur in a strongly acidic medium, may account for the acid-catalyzed aquation reaction:

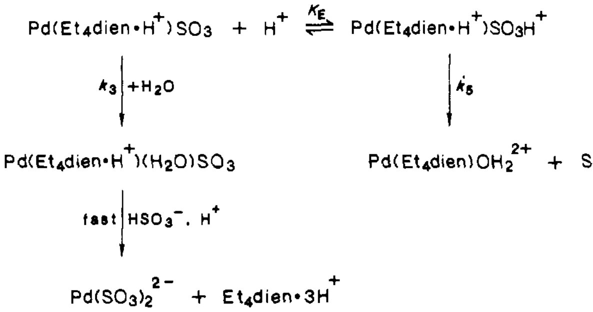

(13)

The overall rate law for this process is

$$k_{obsd} = \frac{k_3 + k_5K_E[H^+]}{1 + K_E[H^+]} \qquad (14)$$

For small values of K_E, $1 + K_E[H^+] \sim 1$ and eq 14 simplifies to $k_{obsd} = k_3 + k_5K_E[H^+]$. From the plot in Figure 6 it follows that $k_3 = (5.2 \pm 0.4) \times 10^{-3}$ s^{-1} and $k_5K_E = (2.7 \pm 0.2) \times 10^{-3}$ M^{-1} s^{-1}. K_E is expected to be small, in agreement with what we have found for the protonation of octahedral sulfito complexes.[2,12] The linearity of the k_{obsd} vs. $[H^+]$ plot indicates that our selected acidity range is still far away from the saturation achieved when the sulfito complex is fully protonated as in the case of carbonato complexes. Acid-catalyzed aquation of carbonato complexes also exhibited a higher acidity constant for the square-planar system than for the octahedral ones, and a similar trend seems to be present in the case of the sulfito complexes. The k_5 reaction path can involve an associative solvolysis process, in which the bisulfite complex is more labile than the sulfite complex, or elimination of SO_2, during which the Pd–O bond remains intact. Such reactions have clearly been found to occur in the case of octahedral O-bonded sulfto complexes. At low $[H^+]$, eq 14 reduces to $k_{obsd} = k_3$, which is exactly the case observed in Figure 5. The doubly protonated $Pd(Et_4dien{\cdot}H^+)SO_3H^+$ species does not undergo dechelation as shown by the fact that, in highly acidic medium, aquation is the only observed process. This can be explained in terms of the weaker labilization effect of bisulfite as compared to that of sulfite, which presumably significantly affects the ring-opening step of the amine ligand.

Simultaneous Formation and Decomposition of $Pd(Et_4dien)SO_3$. We have already mentioned (see also part 1) that the anation of $Pd(Et_4dien)OH_2^{2+}$ by HSO_3^-/SO_3^{2-} at pH <7 results in the subsequent dechelation process and the formation of $Pd(SO_3)_2^{2-}$. Kinetic measurements at the isosbestic point for the second reaction enabled us to gain insight into the mechanism of the anation step. Similarly, the kinetics of the second reaction can be followed under these conditions by measuring the absorbance increse at 365 nm starting from the moment that the isosbestic point is formed at 262 nm, i.e. at the point where the second step is the rate-determining process. Such data should correspond to those measured via the pH-jump technique employed in the previous section. However, there is a fundamental difference in that only partial formation of the $Pd(Et_4dien)SO_3$ species occurs in the present case. In the pH-jump procedure the sulfito complex is fully formed at pH >8 before the solution is acidified to observe the dechelation step. In this respect it is important to note that the extent to which the $Pd(Et_4dien)SO_3$ complex is produced, under conditions where the dechelation reaction interferes, strongly depends on the pH and [total S] (see earlier discussion).

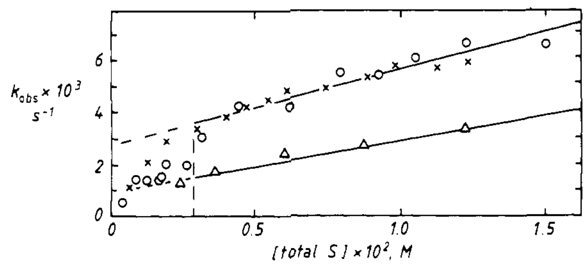

Figure 7. Dependence of k_{obsd} on [total S] at different pHs for the formation of $Pd(SO_3)_2^{2-}$ with $Pd(Et_4dien)OH_2^{2+}$ as starting material. Conditions: [Pd] = 8.7×10^{-5} M; temperature 25 °C; ionic strength 0.5 M; pH 3.3 (○), 4.2 (×), and 6.0 (△).

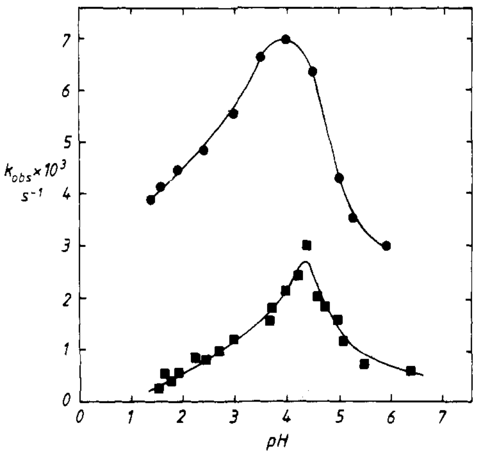

Figure 8. Dependence of k_{obsd} on pH at different [total S] for the formation of $Pd(SO_3)_2^{2-}$ with $Pd(Et_4dien)OH_2^{2+}$ as starting material. Conditions: [Pd] = 8.7×10^{-5} M; temperature 25 °C; ionic strength 0.5 M; [total S] = 1.2×10^{-3} (■) and 1.2×10^{-2} M (●).

The results obtained are summarized in Figures 7 and 8. The observed rate constant partly exhibits the same trends as those observed with the pH-jump technique (Figures 4 and 5). The dechelation rate constant increases with increasing [total S] (Figure 7), and the data at pH 3.3 and 4.2 exhibit the same trend as in Figure 4 for [total S] > 2.7×10^{-3} M. The slope of this line (k_4) is 0.29 ± 0.02 M^{-1} s^{-1}, which is in good agreement with the slope of 0.30 ± 0.03 M^{-1} s^{-1} reported in Figure 4. Similarly, all the data points at pH 6.0 are in good agreement (slope = 0.21 ± 0.02 M^{-1} s^{-1}) with those reported in Figure 3 (slope = 0.22 ± 0.02 M^{-1} s^{-1}). However, there are quite a few data points in the lower [total S] range at pH 3.3 and 4.2 that deviate from the expected trend and do not exhibit the intercept found in Figure 4. This can be understood in terms of the partial formation of $Pd(Et_4dien)SO_3$ under such conditions, so that the subsequent reaction will be affected by the further formation of this species. Under conditions where this species is produced rapidly, i.e. high pH and [total S], the subsequent reaction exhibits kinetics similar to those observed with the pH-jump technique. In this respect it is important to note that k_{obsd} for the dechelation step was found to be proportional to the extent to which the $Pd(Et_4dien)SO_3$ complex is formed, as reflected by the absorbance at the isosbestic point (details are given in ref 18). It follows that this proportionality can account for the increase in k_{obsd} with increasing [total S] under conditions where the intermediate sulfito complex is only partially produced.

The pH dependencies reported in Figure 8 can be interpreted in a similar way. The decrease in k_{obsd} with increasing pH at pH >4 coincides exactly with that reported in Figure 5 and ref 2. The significant pH dependence at pH <4, where Figure 5 exhibits no meaningful dependence, is ascribed to the partial formation of the $Pd(Et_4dien)SO_3$ complex as also reflected by the spectral measurements at the isosbestic point.[18] We conclude that the trends observed during the simultaneous formation and decomposition of Pd(Et_4dien)SO_3 are in good agreement with the results obtained under conditions where these reactions can be studied separately.

The kinetic data of this paper allow us to propose reaction mechanisms for the various steps that are in agreement with the observations of part 1 of this study and with our general understanding of such systems. The sulfite ligand exhibits a unique behavior, which can be related to the properties of S-bonded species. Similar dechelation reactions were also observed recently in anation reactions of closely related complexes with thiosulfate, thiourea, and substituted thioureas.[29]

Acknowledgment. We gratefully acknowledge financial support from the Deutsche Forschungsgemeinschaft and the Fonds der Chemischen Industrie and a loan of $PdCl_2$ from Hereaus GmbH, Hanau, West Germany.

Registry No. Pd(Et_4dien)OH_2^{2+}, 20130-53-4; SO_3^{2-}, 14265-45-3; Pd(Et_4dien)SO_3, 23151-69-1.

Contribution from the Department of Chemistry,
University of Victoria, Victoria, BC, V8W 2Y2 Canada

Kinetics and Mechanism of the Reduction of Nickel(III) Macrocyclic Complexes by Iodide Ion

M. G. Fairbank and A. McAuley*

Received October 5, 1986

The kinetics of reduction of several nickel(III) tetraaza macrocyclic complexes by iodide ion have been measured in perchlorate media. Over a large range (up to 400-fold excess) of I^- concentrations, the reaction order is unity with respect to both [$Ni^{III}L$] and [I^-]. For L = *C-rac*-5,12-dimethylcyclam, two processes are observed, complex formation, $k_f = 2.9 \times 10^4$ M^{-1} s^{-1}, followed by a redox step, $k_4 = 5.5 \times 10^3$ M^{-1} s^{-1}, both of which are iodide-dependent. In the reaction with Ni^{III}tet-c^{3+}, a redox equilibrium is again postulated. Differences in reactivity are attributed to varying stereochemistries of the substituents on the macrocyclic ring. Comparisons with other outer-sphere reactions of iodide indicate that the processes under investigation are inner sphere in nature. The mechanisms of iodide oxidation encountered in Ni(III)–peptide and Cu(III)–peptide complexes are compared with those observed in the present investigation, where axial ligand binding is stronger.

Introduction

Redox reactions of nickel(II/III) macrocyclic complexes continue to be the subject of study.[1-3] Relatively few detailed investigations of oxidations by nickel(III) macrocycles have been made, since reactions may be either outer or inner sphere depending on the substitution lability of the axially coordinated solvent molecules on the metal center. Largely on the basis of a comparison of ligand-exchange rates and reaction rates, reductions of Ni(III) macrocycles by $TiOH^{2+}$,[4] Fe^{2+}, and VO^{2+} [5] have all been assigned as outer-sphere processes. For nickel(III) peptide complexes, which are more axially labile than the nickel(III) macrocycles,[6] an inner-sphere process has been postulated.[7]

Reduction of nickel(III) macrocycles by iodide ion was first described in 1979[8] in a pulse-radiolytic and flash-photolytic study of nickel(II/III) systems. Unfortunately, the kinetics of the process could not be investigated, owing to preferential oxidation of I^- by the radicals used to generate the nickel(III) complexes. In the kinetics of reduction of Ni^{III}cyclam^{3+} by I^-,[9] the reaction was found to be first order in both [I^-] and [Ni(III)] and an outer-sphere mechanism was tentatively assigned. More recently[10] similar concentration dependences have been observed in the oxidation with Ni(9-aneN_3)$_2^{3+}$, which is known to react as an outer-sphere reagent. In contrast, the kinetics of the reaction of I^- with the nickel(III) complex of tri-α-aminoisobutyric acid Ni(H_{-2}Aib$_3$) have been shown[11] to proceed via a major pathway second order in both [I^-] and [Ni(III)]. This was attributed to the formation of a iodonickel(III) complex and subsequent rate-determining reaction of two such species to form I_2 and two Ni(II) peptide species directly in a concerted two-electron transfer. A second minor route, first order in [Ni(III)] and second order in [I^-], involved reaction of the monoiodide species with I^- to yield I_2^-, which on further rapid oxidation with Ni(III) yielded I_2.

Slightly different behavior was observed in the reaction of iodide with several copper(III) peptide complexes. At higher concentrations of I^-, the behavior was similar to the minor [I^-]^2 pathway of the nickel(III) systems. However, at lower [I^-] the order of unity in both oxidant and reductant was consistent with a pathway in which $I^\bullet$ was produced, which reacted rapidly either with Cu(III) or with $I^\bullet$ to give I_2. The differences in reaction behavior can be attributed[11] to the nature of the axial lability in the complexes. As has been shown, the peptide–iodonickel(III) species is formed readily, whereas for Cu(III) complexes, which are square planar, any association with the iodide may be an ion pair rather than an axially substituted (inner sphere) ion.

In this paper, the kinetics of reaction of several nickel(III) tetraaza macrocyclic complexes with I^- are reported. Over the concentration ranges used (10–400-fold excess of reductant) there is evidence for only one pathway with a first-order dependence on both [$Ni^{III}L^{3+}$] and [I^-].

Experimental Section

The nickel(II) complexes [NiM_m](ClO_4)$_2$ (M_m = α-*C-meso*-5,12-dimethyl-1,4,8,11-tetraazacyclotetradecane),[12] [NiM_r](ClO_4)$_2$ (M_r = *C*-

---

(1) Jaacobi, M.; Meyerstein, D.; Lilie, J. *Inorg. Chem.* **1979**, *18*, 429.
(2) Brodovitch, J.-C.; McAuley, A.; Oswald, T. *Inorg. Chem.* **1982**, *21*, 3442.
(3) Macartney, D. H.; Sutin, N. *Inorg. Chem.* **1983**, *22*, 3530.
(4) McAuley, A.; Olubuyide, O.; Spencer, L.; West, P. R. *Inorg. Chem.* **1984**, *23*, 2594.
(5) Macartney, D. H.; McAuley, A.; Olubuyide, O. *Inorg. Chem.* **1985**, *24*, 307.
(6) Murray, C. K.; Margerum, D. W. *Inorg. Chem.* **1982**, *21*, 3501.
(7) Owens, G. D.; Phillips, D. A.; Czarnecki, J. J.; Raycheba, J. M. T.; Margerum, D. W. *Inorg. Chem.* **1984**, *23*, 1345.
(8) Whitburn, K. D.; Lawrence, G. S. *J. Chem. Soc., Dalton Trans.* **1979**, 139.
(9) Haines, R. I.; McAuley, A. *Inorg. Chem.* **1980**, *19*, 719.
(10) McAuley, A.; Norman, P. R.; Olubuyide, O. *Inorg. Chem.* **1984**, *23*, 1938.
(11) Raycheba, J. M. T.; Margerum, D. W. *Inorg. Chem.* **1981**, *20*, 1441.
(12) Raycheba, J. M. T.; Margerum, D. W. *Inorg. Chem.* **1981**, *20*, 45.